

Journal of Materials Chemistry A

Accepted Manuscript



This is an *Accepted Manuscript*, which has been through the Royal Society of Chemistry peer review process and has been accepted for publication.

Accepted Manuscripts are published online shortly after acceptance, before technical editing, formatting and proof reading. Using this free service, authors can make their results available to the community, in citable form, before we publish the edited article. We will replace this *Accepted Manuscript* with the edited and formatted *Advance Article* as soon as it is available.

You can find more information about *Accepted Manuscripts* in the [Information for Authors](#).

Please note that technical editing may introduce minor changes to the text and/or graphics, which may alter content. The journal's standard [Terms & Conditions](#) and the [Ethical guidelines](#) still apply. In no event shall the Royal Society of Chemistry be held responsible for any errors or omissions in this *Accepted Manuscript* or any consequences arising from the use of any information it contains.

FEATURE ARTICLE

Graphene Derivatives**Graphane, fluorographene, graphene oxide, graphyne and graphdiyne**Michio Inagaki*^a and Feiyu Kang^b

^a Professor Emeritus of Hokkaido University, 228-7399 Nakagawa, Hosoe-cho, Kita-ku, Hamamatsu 431-1304, Japan. E-mail: im-ii@ace.ocn.ne.jp

^b Dean and Professor of Graduate School at Shenzhen, Tsinghua University, University Town, Shenzhen, Guangdong 518055, China

New carbon materials have recently been derived from graphene theoretically and experimentally, hydrogenated graphene (graphane), fluorinated graphene (fluorographene), oxidized graphene (graphene oxide), graphene introduced by acetylenic chains (graphyne and graphdiyne), which may call graphene derivatives. Here, we review these graphene derivatives by emphasizing the experimental results.

1. Introduction

Since the first proposal of the term "graphene" in 1986¹, numerous theoretical and experimental research works on graphene and graphene-like materials have been reported. Research activity is obviously accelerated by the fact that Nobel Prize in physics has been given to Profs. A. K. Geim and K. S. Novoselov for their pioneering works on graphene in 2010². Rapid increase in scientific and technological interests on graphenes causes some confusion of the definition and terminology for graphene-related materials even in scientific journals. A proposal on the nomenclature for two-dimensional carbon materials has recently been presented in Journal CARBON³.

Recently, hydrogenated, fluorinated and oxidized graphenes are expected to have interesting properties, which are called graphane, fluorographene and graphene oxide, respectively. In addition, the introduction of either acetylenic or diacetylenic chains between carbon hexagons is experimentally shown to give the layer of single-atom thickness, which is flat as graphene and is predicted to have interesting properties as graphene has; the former is named graphyne and the latter graphdiyne. Graphyne and graphdiyne cannot be prepared directly from graphene, but they are compared and discussed with graphene in respect to their structure and properties. In this review, therefore, they are classified as graphene derivatives, together with graphane, fluorographene and graphene oxide. On graphene-related nanomaterials, including doped graphene, graphene nanoribbons, porous graphene in addition to five nanomaterials which we classified as graphene derivatives, are recently reviewed⁴. Here, we presented the review focusing the graphene derivatives by emphasizing the experimental results. Graphene is not the theme of this review because many comprehensive reviews have already been published from different viewpoints⁵.

2. Hydrogenated graphene (graphane)

Fully hydrogenated derivative of graphene, of which chemical composition is CH, is predicted on the basis of first-principles total energy calculations⁶ and named graphane⁷. It consists of sp³ C-C bonds, as opposed to graphene's sp² bonds, and consequently carbon atom layer is puckered. Graphane can have two conformations, as schematically shown on their top-views in Fig. 1: a chair-like conformer with the hydrogen atoms alternating on both sides of the carbon atom layer and a boat-like conformer with the hydrogen atoms alternating in

pairs. The space group, bond distances and binding energy predicted⁶ are shown for two conformers in Table 1. In chair-type conformer, the calculated C-C bond length of 0.152 nm is similar to that in diamond (sp^3 bonding) and is much greater than that in graphene (0.142 nm characteristic for sp^2 bonding). In boat-type conformer, two different C-C bond lengths are expected, 0.152 and 0.156 nm: the former corresponds to two carbon atoms bonded to hydrogen atoms on opposite sides and the latter to those bonded to hydrogen atoms on the same side, slightly longer than 0.152 nm due to H-H repulsion. The calculated binding energy is 6.56 eV/atom for chair-type and 6.50 eV/atom for boat-type, suggesting the former is favorable. This binding energy calculated for chair-type graphane is even higher than those for other hydrocarbons, such as benzene (6.49 eV/atom) and acetylene (5.90 eV/atom). Therefore, graphane can be considered as an extended two-dimensional hydrocarbon and is the most stable compound with a stoichiometric formula unit CH. Two conformations in graphane is also considered as two-dimensional analogs of diamond, chair-type to cubic diamond and boat-type to hexagonal one. Similar calculation on graphane has been performed in comparison with fluorographite⁸. Calculation using *ab initio* and classical molecular dynamics methods suggested the presence of the domains with hydrogen frustration (breaking the H atoms up and down alternating pattern) in graphane, particularly in the early stages of the hydrogenation⁹. The stability of three-dimensional crystals built up from two-dimensional graphane sheets under pressure up to 300 GPa is explored¹⁰.

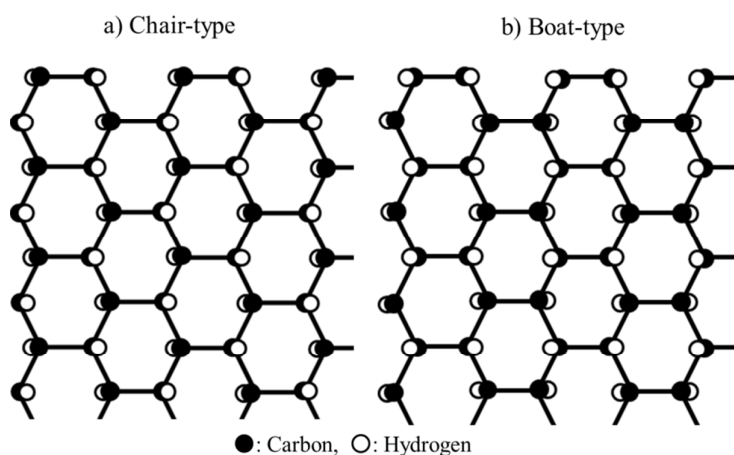


Fig. 1 Structure of graphane (top view): (a) chair-type and (b) boat-type conforms.

Table 1 Crystal parameters for two conformations of graphane predicted. Reproduced from ref. 7 with permission.

Graphane conformation	Space group	Bond length (nm)		Binding energy (eV/atom)
		C-C	C-H	
Chair-type	$P-3m1$	0.152	0.111	6.56
Boat-type	$Pmmn$	0.152 & 0.156	0.110	6.50

Graphane was firstly synthesized in 2009 by exposing graphene to cold hydrogen plasma using argon mixed with 10 % hydrogen at a low-pressure 10 Pa and a temperature of 4-160 K¹¹. Hydrogenation transforms highly conductive zero-overlap semi-metallic graphene into insulating graphane, the reaction being reversible by plasma irradiation and annealing. Graphane and graphenes hydrogenated in various extents are formed by electrolytic hydrogenation of thin graphite flakes in water by applying 10.0 V and 2×10^{-3} A at room temperature¹². In Fig. 2, Raman spectrum of graphane (fully hydrogenated) is compared with that of the pristine graphene. Marked development of D-band, broadening of G- and

2D-bands, and appearance of a new band (denoted as E) are characteristic for graphane, the developments of D-band and E-band being correlated to hydrogen content. Change in Raman spectrum with exposing time under radio frequency hydrogen plasma (13.56 MHz, 300 W) in ultrahigh-vacuum is observed on single-layer graphene, as shown in Fig. 3¹³. Intensity of D-band gradually increases and the change seems to be saturated after 50 sec exposure. Exfoliation of graphite oxide under high hydrogen pressure (6-15 MPa and 200-500 °C) gave partially hydrogenated graphenes^{14,15}. It was theoretically shown that hydrogen atoms on one side of graphane can be unloaded by applying an external electric field, where the hydrogen atoms on the other side are kept and the unpaired electrons in the unsaturated C sites give rise to magnetic moments¹⁶. Hydrogen treatment at higher temperature and pressure (400-550 °C and 5 MPa) results in the partial hydrogenation of single-wall carbon nanotubes (SWCNTs), some being unzipped into partially-hydrogenated graphene nanoribbons at 550 °C¹⁷.

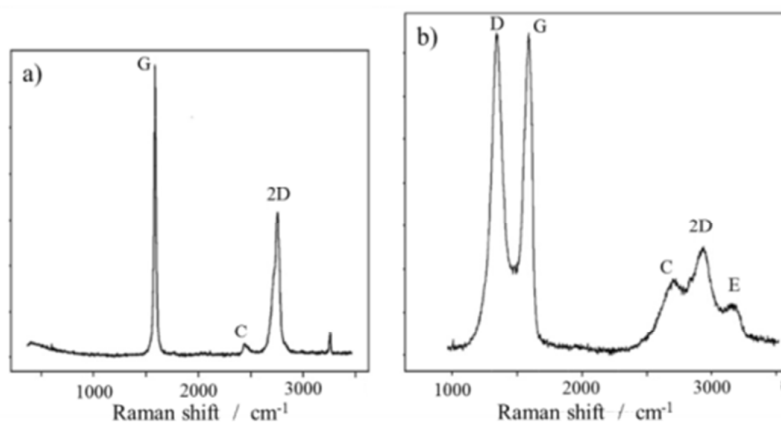


Fig. 2 Raman spectra of the pristine graphite thin flake (a) and after fully-hydrogenated (graphane) (b). Reproduced from ref. 12 with permission of Elsevier.

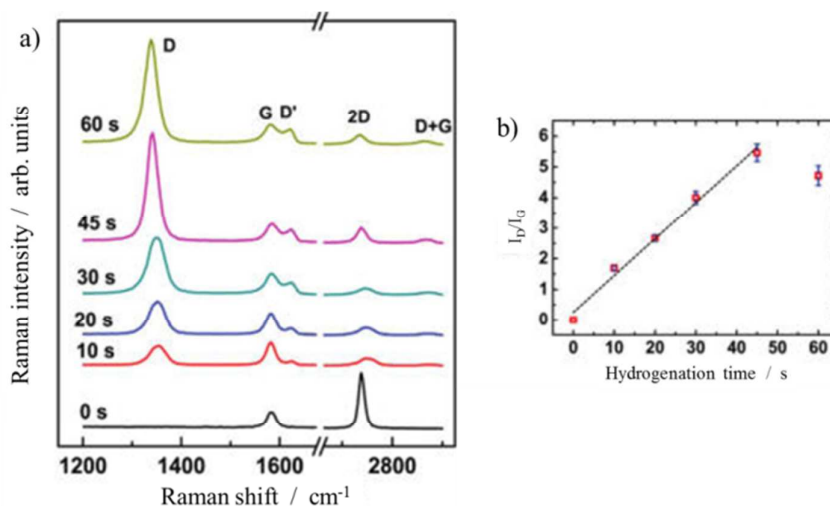


Fig. 3 Changes in Raman spectrum (a) and I_D/I_G ratio (b) for single-layer graphene with hydrogenation time. Reproduced from ref. 13 with permission of American Chemical Society.

Opening of band gap of graphene with hydrogenation was studied on a sheet grown on the (111) surface of Ir crystal, suggesting a possibility to tune the band gap by partial hydrogenation¹⁸. Band gap increases gradually with increasing hydrogenation degree,

reaching to 0.77 eV when 54 % of the carbon atoms are bonded to hydrogen to form graphane-like islands. The electronic properties of graphene sheets and nanoribbons hydrogenated in different degrees under hydrogen plasma have been studied¹³. Marked effect of hydrogenation is observed on the dependence of resistance R on back-gate voltage V_{bg} for graphene nanoribbons, as shown in Fig. 4. Maximum value of R increases rapidly with increasing exposure time, i.e., increasing hydrogenation degree, together with the increase in V_{bg} appearing R maximum. Rapid decrease in the mobility of carriers is also observed with hydrogenation.

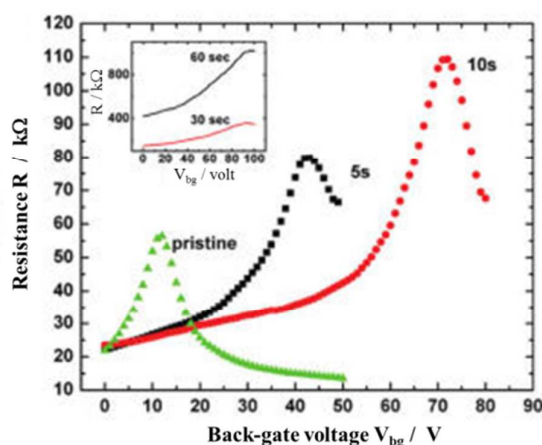


Fig. 4 Change in the dependence of resistance R on back-gate voltage V_{bg} for graphene nanoribbons as a function of exposure time for hydrogen plasma. Reproduced from ref. 13 with permission of American Chemical Society.

Interesting properties have been predicted by theoretical calculations for graphane and partially-hydrogenated graphenes. In graphane the thermal energy can be accommodated by in-plane bending modes, involving C-C-C bond angles in the puckered carbon layer, in contrast to significant out-of-plane fluctuation modes in graphene¹⁹. Thermal properties of graphane up to 1500 K were predicted using simulation, heat capacity being 29.32 J/molK, a little larger than graphene²⁰. Graphane has a lower hydrophobicity compared to graphene²¹. The minimum band gap is 5.4 eV in the stable chair-type conformation, and 4.9 eV in the metastable boat-type conformation²². Gradual increase in band-gap with hydrogenation was theoretically predicted, from 0 eV for graphene to 4.4 eV for graphane (fully-hydrogenated)¹¹. The electronic and magnetic properties were discussed on the bases of theoretical calculations for graphane nanoribbons²³. Hydrogenation from graphene to fully-hydrogenated graphane was predicted to cause the change in electronic and magnetic properties from metallic to semiconducting and from nonmagnetic to magnetic²⁴. H-vacancy defects induced on one side of the graphane are found to be the source of ferromagnetism even at room temperature²⁵. For the nanoribbons having the zigzag interfaces between graphene and graphane domains, it is predicted that the nanoribbon behaves antiferromagnetic when interfaces are fully hydrogenated, and ferromagnetic when half hydrogenated²⁶. Graphane doped by alkali-metal atoms at the low concentration of 3.125 % shows semiconductor behavior, whereas at high concentration the doped graphane shows metallic behavior, in contrast to the prediction that graphane doped by alkaline-earth metals exhibits metallic behavior at all doping concentrations²⁷. The optical properties of graphane are dominated by localized charge-transfer excitations governed by enhanced electron correlations in a two-dimensional dielectric medium²⁸. Substitution of B, N, P, and Al atoms for carbon atoms in graphane can cause the transition from semiconductor to metal²⁹. Li-doped graphane can achieve a

hydrogen storage capacity of 3.2-3.8 mass%^{30,31}.

Theoretical consideration was also applied on graphene nanotubes³² and nanoribbons³³. Armchair type nanotube from chair-type graphane, shown in Fig. 5, was the most stable configuration among the nanotube structures considered, even at elevated temperature³². The calculated band gaps of graphane nanotubes depended on both the diameter and hydrogenation degree of the nanotube, suggesting insulating behaviors of nanotubes.

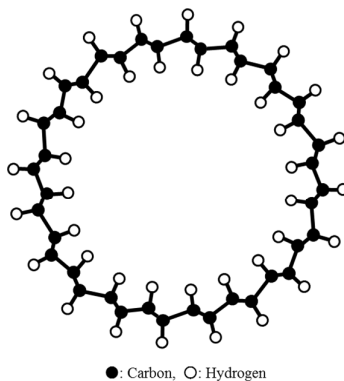


Fig. 5 Graphane nanotube built from chair-type graphane. Reproduced from ref. 30 with permission.

3. Fluorinated graphene (fluorographene)

The reaction of graphite with fluorine has been studied already in 1934^{34,35}. The structure and chemical composition of graphite fluorides represented by $(CF)_n$ and $(C_2F)_n$ are well understood, and definite applications as anode material of lithium primary batteries and super-hydrophobic material³⁶. In graphite fluorides with the composition CF and C_2F , the graphite layers are no longer flat but puckered in chair-type. In C_2F , half of the carbon atoms form covalent bond with fluorine and the other half are also covalently bonded with carbon atoms in neighbouring layers.

Fluorinated graphene (fluorographene), monolayer of graphite fluoride, is another important structural derivative of graphene. Structure of fully-fluorinated graphene has chair-type conformation, similar to graphane. Boat-type conformation is supposed to be difficult to be formed in fluorographene, because fluorine atoms alternating on one side of the carbon atom layer in pairs give strong repulsion. Fluorographene has been synthesized by reacting graphene with either XeF_2 ³⁷⁻³⁹ and CF_4 ⁴⁰ at room temperature, and by mechanical and chemical exfoliation of graphite fluoride^{41,42}. The methods announced for the synthesis in large-scale process with a low cost and less toxicity have also been proposed; sonochemical exfoliation process of graphite fluoride in N-methyl-2-pyrrolidone (NMP) at room temperature⁴³ and reaction of graphene oxide with HF under hydrothermal condition with ultrasonication⁴⁴.

Fluorographene synthesized by heating graphene in XeF_2 gas at 250 °C has a band gap of 3.8 eV, close to that calculated, and cannot be suspended in ethanol, although the pristine graphene can be suspended by sonication for 30 s, as shown in Fig. 6³⁹. It luminesces in the UV and visible light regions, and resembles diamond in its optical properties, with both excitonic, and direct optical absorption and emission features. Fluorographene, which is prepared by the reaction of graphene with XeF_2 gas at 70 °C, is a high-quality insulator (resistivity of higher than $10^{12} \Omega$) with an optical gap of 3 eV, exhibits a Young's modulus of 100 N/m, and is stable up to 400 °C even in air, similar to Teflon³⁷. By exposure of one side of graphene to XeF_2 gas, fluorination was saturated at 25 % coverage (composition of C_4F), although full coverage (CF) was attained by both-sides exposure³⁸. In Fig. 7, Raman spectra

are shown for partially-fluorinated graphene prepared by exposing to CF_4 plasma at room temperature and de-fluorinated graphene at 365°C in $\text{Ar}+\text{H}_2$ gas, revealing that marked change in D- and 2D-bands by fluorination and de-fluorination⁴⁰. Dilute fluorination of graphene results in a temperature dependence as insulator and the resistance at the charge neutrality point increases by three orders of magnitude from 25 k Ω at 200 K to 2.5 M Ω at 5 K, although pristine graphene is highly conductive with a weak temperature dependence of resistance. Fluorographene was obtained as supernatant by exfoliation of graphite fluoride in sulfolane under sonication at 50°C for 1 h, consisting of single-layer fluorographene with the thickness of less than 0.9 nm in a significant fraction, together with multilayered sheets of about 2-4 nm thickness⁴¹. Its de-fluorination was possible in sulfolane solution of KI by heating under stirring at 240°C for 2 h, the process being supposed to proceed via the formation of metastable graphene iodide. Comparative quantum mechanical calculations reveal that fluorographene is the most thermodynamically stable of five hypothetical graphene derivatives; graphane, graphene fluoride, bromide, chloride, and iodide.

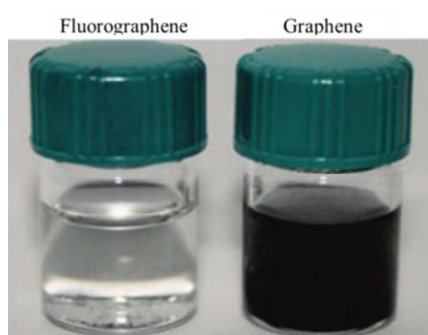


Fig. 6 Dispersed state of fluorographene and graphene in ethanol. Reproduced from ref. 39 with permission of American Chemical Society.

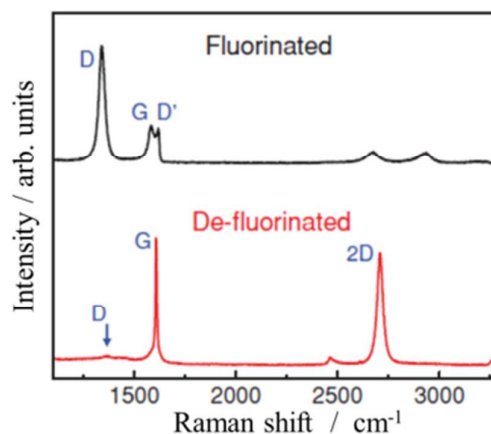


Fig. 7 Raman spectrum of partially-fluorinated and de-fluorinated graphene. Reproduced from ref. 40 with permission.

Theoretical predictions of the properties of fluorographene by comparing with graphane, because of their similar bonding states and of their applications, have been published⁴⁵⁻⁵¹. Fluorographene exhibits much lower friction than graphane, as shown by plotting energy corrugation with displacement in Fig. 8, because of the low interlayer interaction induced by the repulsive electrostatic forces between F^{50} . Doping of fluorographene with K, Li, Au and $\text{C}_{12}\text{N}_4\text{F}_4$ is studied by density functional theory (DFT), showing that the former two act as

electron donor (n-type doping) but the latter two suggest difficulty of p-type doping in fluorographene⁴⁶. Doping of boron substituting carbon atoms in fluorographene seems to occur easily and create shallow acceptor level, while nitrogen act as deep donors in chemically unstable system⁴⁹. The process of fluorination of graphene in fluorine and also in mixed gases of fluorine with hydrogen is theoretically studied⁴⁷. Fluorination tends to produce defective areas on graphene, being associated with large holes, due to significant distortion of carbon-carbon bonds⁵¹. The presence of a small amount of hydrogen in fluorine gas causes a significant decrease in the rate of fluorination, while hydrogen incorporation into graphene is accelerated by the presence of small amount fluorine in hydrogen gas. Formation of new hybrid structures containing hydrogen and fluorine with different stable configurations (chair-, zigzag- and boat-types) are predicted, as shown in Fig. 9.

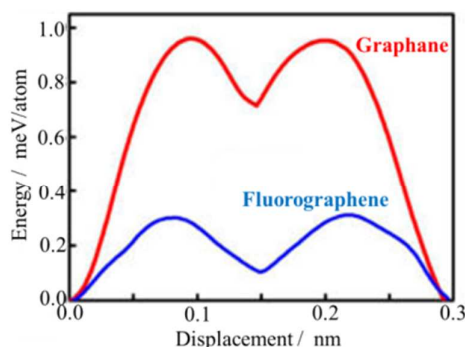


Fig. 8 Variation of the energy corrugation of the fluorographene and graphane with the sliding displacement. Reproduced from ref. 50 with permission.

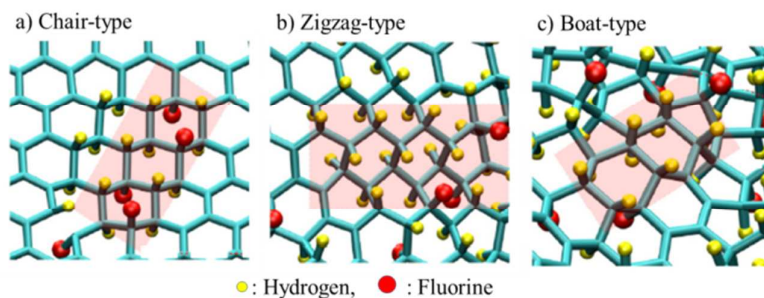


Fig. 9 Hybrid structure by the reaction with hydrogen/fluorine mixed gas. Reproduced from ref. 51 with permission of IOP publishing.

Partially fluorinated graphenes were obtained by exfoliation of graphite fluorides with F/C ratio of 0.25 and 0.5 in an ionic liquid (1-butyl-3-methylimidazolium bromide) under ultrasonication⁴². DFT calculation showed that the band gap of fluorinated graphene depends sensitively on the coverage and configuration of fluorine atoms. Fluorination of SWCNTs was successfully performed in F₂/He gas at the temperature below 325 °C by keeping tube-like morphology with a composition close to C₂F⁵², suggesting almost complete coverage of the outer surface of nanotubes by fluorine. Very low friction coefficient was confirmed on fluorinated SWCNTs⁵³.

4. Oxidized graphene (graphene oxide)

In most cases, graphite oxide was synthesized using the process proposed by Hummers and Offeman⁵⁴ which was derived from the method of Staudenmaier⁵⁵, often called Hummers

method. Its principal steps are the oxidation of graphite in concentrated H_2SO_4 with NaNO_3 and KMnO_4 , the exclusion of excess KMnO_4 by reducing to water-soluble MnSO_4 with H_2O_2 and then washing by methanol. In some attempts the Brodie method⁵⁶ was used, where the oxidation of graphite was carried out in fuming HNO_3 with KClO_3 . To synthesize graphite oxide, the electrochemical oxidation of graphite can be applied in either H_2SO_4 or HNO_3 ^{57,58} and also in an ammonia solution⁵⁹. Improved method by using $\text{H}_2\text{SO}_4/\text{H}_3\text{PO}_4$ mixture was recently proposed, saying the advantages of high yield of graphite oxide, easiness of reaction temperature control and no generation of toxic gases⁶⁰. Formation process of graphite oxide from graphite was discussed by dividing into three steps, conversion to intercalation compounds, oxidation by inserting the oxidizing agent into the preoccupied graphite galleries, and exposure to water resulting in losing c-axis order⁶¹. The second step is entirely diffusion-controlled process, consequently rate-determining. Graphite oxide contains oxygen and hydroxide radicals in various amounts making covalent bonds with carbon and, as a consequence, layer of carbon atoms is not flat. Graphite oxides synthesized can have a wide range of chemical compositions, such as $\text{C}_8\text{O}_{3.5-4.3}\text{H}_{2.5-2.9}$ ⁶², $\text{C}_8\text{O}_{3.78-5.05}\text{H}_{2.9-4.4}$ ⁶³, $\text{C}_8\text{O}_{2.54}\text{H}_{3.91}$ and $\text{C}_8\text{O}_{4.61}\text{H}_{6.70}$ ⁶⁴, depending strongly on the starting graphite and the synthesis conditions, and also containing different kinds of oxygen species and bonds to carbon, such as epoxy, hydroxyl, carbonyl, carboxylic groups. On graphite oxides synthesized from flaky graphite via Brodie method, marked color change from grey to gold was observed, probably because of the change in oxygen-containing radicals, but no marked changes in bulk chemical composition and interlayer spacing with repetition of oxidation process⁶⁵. Structure models proposed by different authors are shown in Fig. 10. Graphite oxide has been used as host materials for intercalation compounds with different linear organic compounds⁶⁶⁻⁷⁰. Various trimethylammonium cations can be intercalated into the gallery of graphite oxide with different orientations of long linear molecules⁶⁷.

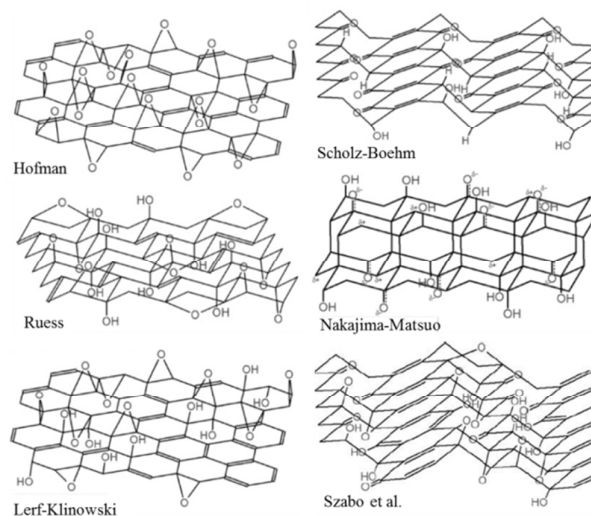


Fig. 10 Proposed structure of graphite oxides.

Graphene oxide is a single layer sheet of graphite oxide. In recent years, it has attracted great concern mainly because it is a potential starting materials for the mass production of graphene⁵. Chemistry of graphene oxide has been reviewed⁷¹.

Graphene oxide can be semiconductor or insulator, depending on the degree of oxidation, and their electronic and optical properties can be tuned in a wide range. The controllable optical and electronic properties enable graphene oxides to be used in many fields. The

major concern about graphene oxide is mainly focused on its chemical structure, electronic properties, reduction reaction and chemical functionalization.

Graphene films grown epitaxially on the C-terminated surface of a SiC wafer were converted to multilayer graphene oxide via the Hummers method, of which stability with aging time at room temperature were studied from the measurement of XPS spectrum⁷². As-prepared graphene oxide is metastable, of which the contents of oxygen and graphene oxide decrease gradually even after 1 month, and then the change tends to be saturated. Atomic and electronic structures of graphene oxide were studied by TEM, AFM and electron energy loss spectroscopy (EELS)⁷³. In Fig. 11, AFM image of graphene oxide prepared by oxidation (Hummers method) of graphene (Fig. 11a) and its depth intensity histograms (Fig. 11b), showing that the particles consist of mono-, bi- and tri-layers are easily observed. In Fig. 11c), EELS spectrum, which is a direct measure of the dielectric response of the film to the external electromagnetic excitation, is shown for a mono-layer graphene oxide comparing with graphite and amorphous carbon. The peak for bulk plasma-loss (combination of π^* and σ^* electronic excitations) occurs at 24-27 eV for graphite and amorphous carbon, but that for graphene oxide does much lower at 19 eV. The low-energy plasma excitations of the π^* electrons, however, occurs at around 5 eV for graphene oxide, similar for graphite and amorphous carbon. Graphene oxide is rough, with an average surface roughness of 0.6 nm, and the structure is predominantly amorphous due to distortions from sp^3 C-O bonds. Around 40 % sp^3 bonding was found to be present in these sheets with O/C ratio of 1/5.

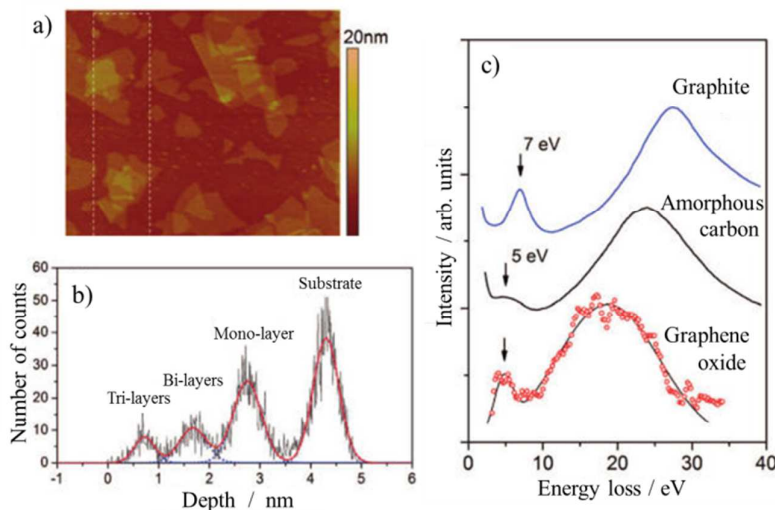


Fig. 11 AFM image (a), AFM depth intensity histograms (b) and low-loss EELS spectrum of graphene oxide (c). Reproduced from ref. 73 with permission.

Many studies have been devoted to prepare graphene oxide sheets having well-controlled thickness and area, and to their reduction to fabricate graphene sheets⁷⁴⁻⁸¹. In the presence of poly(sodium 4-styrenesulfonate), graphite oxide can undergo complete exfoliation in water, yielding colloidal suspensions of almost entirely individual graphene oxide sheets⁸². By filtration of this colloidal suspension through a membrane filter, followed by air drying, graphene oxide film was prepared⁷⁴. The thickness of the film was controlled by adjusting the volume of the colloid. Graphene oxide hydrosol prepared from natural graphite flakes by oxidation was heated at 60 °C for a short period in a water bath to obtain the film on the surface of the aqueous dispersion (on air/water interface), which was collected on a PET substrate by dip coating⁸⁰. To prepare transparent conductive films of graphene oxide, the films were dipped in a HI aqueous solution (55%) at 100 °C for 30 s, and then washed

repeatedly with ethanol to remove the residual HI. Transparent sheets with a large area up to $4 \times 10^4 \mu\text{m}^2$ were successfully prepared. The films after the reduction in HI solution showed a sheet resistance of $840 \Omega/\text{sq}$ by keeping 78 % transparency. Transparent graphene oxide films before and after the reduction in HI aqueous solution are shown in Fig. 12. Reduction of graphene oxide sheets by keeping their structure and texture was reviewed by focusing on the preparation of graphene⁸¹. The electronic properties of graphene oxide mainly depend on the oxidation level and chemical composition; it can be tailored by removal or addition of certain oxygen groups to adjust the proportion of sp^2 and sp^3 carbon^{83,84}.

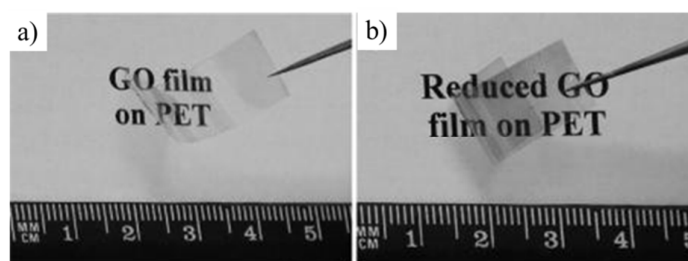


Fig. 12 Transparent films of graphene oxide GO (a) and reduced graphene oxide (b). Reproduced from ref. 80 with permission.

Mechanical properties of graphene oxide were measured on the films prepared by filtration⁷⁴. The stress-strain curve for graphene oxide is divided into three regions, I to III, as shown in Fig. 13a. The region I is due to straightening of the component graphene oxide sheets and shows a residual strain after unloading, as shown in Fig. 13b, which decreases with increasing temperature, supposing to be due to the decrease in water content in the film. The region II is due to elastic deformation and the region III to plastic deformation of the film. The modulus of the film was measured as 32 GPa, increasing slightly with decreasing water content.

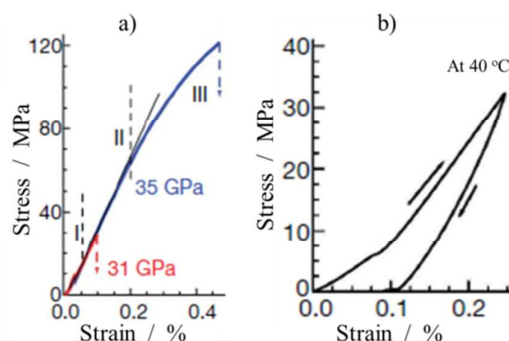


Fig. 13 Stress-strain curves of graphene oxide film with the thickness of $11 \mu\text{m}$: (a) whole curve and (b) loading-unloading in the region I. Reproduced from ref. 74 with permission.

Graphene oxide has attracted increasing interests for drug delivery and other biomedical applications due to its good biocompatibility, ultrahigh drug loading capability, and the ease of surface functionalization⁸⁵⁻⁸⁸. Nano-sized particle of graphene oxide shows superior gene transfection efficiency without serum interference, as well as reduced cytotoxicity, after being physiologically stable dual-polymer-functionalized by using polyethylene glycol and polyethylenimine^{85,86}. Graphene oxide decorated by both iron oxide and gold nanoparticles was coated by polyethylene glycol, obtaining enhanced photothermal cancer ablation effect with high stability in physiological environments and no significant in vitro toxicity⁸⁷. Its

performance was tested in both in vitro cell tests and in vivo animal experiments. Graphene oxide has been pointed out to have distinct advantages as a biosensing platform due to its excellent capabilities for coupling with biomolecules and processing in solution⁸⁹. Biomedical applications for drug delivery, cancer therapies and biomedical imaging were reviewed on graphene oxide and reduced graphene oxide, the behaviours and toxicology of functionalized graphene oxide being discussed⁸⁸. The fact that graphene oxide can contain a large amount of functional groups causes a difficulty for its exact characterization, but it can be an advantage in some applications, particularly in the biomedical applications, because its functionalities are easily modified to improve in an aqueous solution, for example, and new functionalities are expected to be easily created.

5. Graphyne and Graphdiyne

Instead of flat single carbon layer consisting of hexagons (*i.e.*, graphene), as occurred in nature as graphite, flat single atomic layer of carbon is possible by connecting carbon hexagons by linear carbon chains. Graphyne structure, in which carbon hexagons are bonded by linear acetylenic chain, has been predicted in 1987⁹⁰, one year later than the proposal of the definition of "graphene"¹. Later, graphdiyne which consists of two acetylenic chains in between carbon hexagons has been proposed⁹¹. The structures of these two are shown in Fig. 14, by comparing with graphene. The name "graphyne" comes from its chemical structure, one-third of the carbon-carbon bonds in graphene being replaced by acetylenic linkages, and "graphdiyne" from the presence of two acetylenic (di-acetylenic) linkages. The linear carbon chain between carbon hexagons is shown to be more stable to be composed of acetylenic linkages ($\text{—C}\equiv\text{C—}$) than cumulative linkages (=C=C=)⁹².

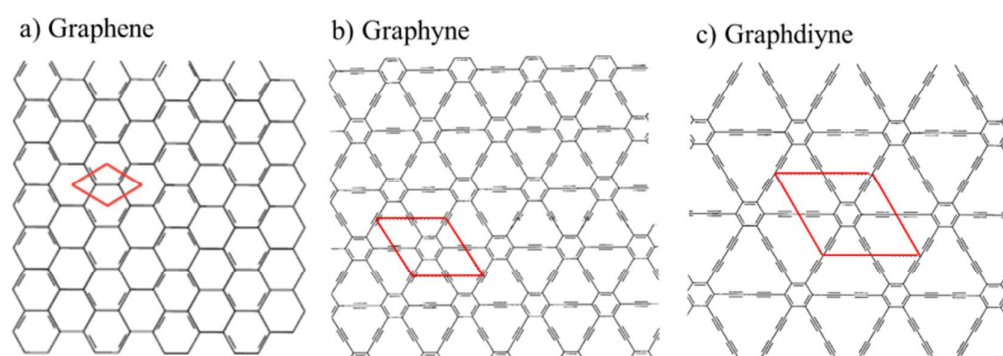


Fig. 14 Structure of graphene (a), graphyne (b) and graphdiyne (c). The parallelogram drawn with a red line represents a unit cell.

Various arrangements of acetylenic linkages to form a flat layer of carbon atoms have been theoretically discussed and reviewed^{93,94}. The two-dimensional arrangements with or without carbon aromatic hexagon, such as Fig. 15a-c, and also numbers of linkages in between two hexagons, as Fig. 15d, are discussed. The binding energy and lattice parameter are 7.95 eV/atom and 0.686 nm for graphyne and 7.78 eV/atom and 0.944 nm for graphdiyne, respectively. Both graphyne and graphdiyne are semiconductive with band gaps of about 0.5-0.6 eV and considerably small effective masses for carriers⁹². The band gap for graphdiyne film is predicted theoretically to be 0.46 eV and its in-plane intrinsic electron mobility can be the order of 10^5 cm²/Vs at room temperature, while the hole mobility is about an order of magnitude lower⁹⁵. Graphyne was predicted to have a Poisson's ratio of 0.417 and an in-plane stiffness of 1036 eV/nm², being much softer than graphene⁹⁶, and Poisson's ratio of 0.429 and in-plane Young's modulus of 162 N/m⁹⁷. Stacking order of

two-dimensional graphdiyne layers was theoretically discussed on the bulk⁹⁸. Thermal conductivity of graphyne was calculated to be much smaller than graphene by assuming different numbers of acetylenic linkage⁹⁹. Mechanical properties of graphyne-like layers, including graphdiyne, were discussed as a function of number of acetylenic linkages^{100,101} and of different arrangements of acetylenic linkages¹⁰². Modulus of graphyne-like layers with zigzag structure is plotted against number of acetylenic linkages in Fig. 16¹⁰¹. For graphdiyne, modulus and ultimate strength were calculated as 470-580 GPa and 36-46 GPa, respectively.

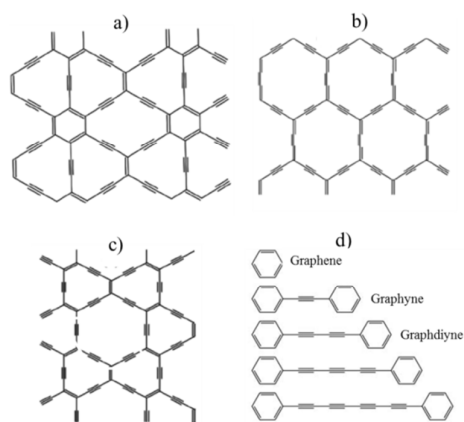


Fig. 15 Various arrangements of acetylenic linkages.

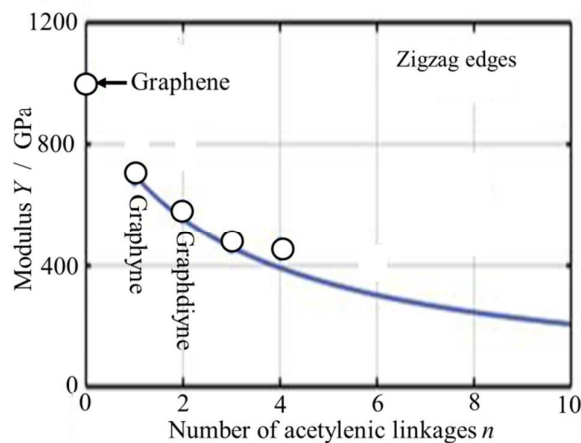


Fig. 16 Modulus of graphyne-like layers as a function of number of acetylenic linkages. Reproduced from ref. 101 with permission.

Substructures of graphyne and graphdiyne have been synthesized^{91,103-110}. Graphdiyne film with a large area ($\sim 3.6 \text{ cm}^2$) has been successfully prepared via cross-coupling reaction of the monomer of hexaethynylbenzene at 60°C in nitrogen atmosphere on copper surface, as shown TEM images and XRD pattern in Fig. 17¹¹¹. The resultant film shows a clear lattice fringe image (Fig. 17b) with spotty selected-area electron diffraction pattern (Fig. 17c) and semiconducting properties. Its XRD pattern gives sharp diffraction peaks (Fig. 17d), interlayer spacing 0.419 nm calculated from the peak at 2θ of 21.18° being the same as calculated from lattice fringe image (Fig. 17b). Graphdiyne is synthesized as nanotube array by using anodic aluminum oxide film template with channel diameter of 200 nm and Cu

catalyst, the nanotubes having the length of about 40 μm and the wall thickness of about 40 nm¹¹². By annealing at 650 $^{\circ}\text{C}$, graphdiyne nanotubes are shrank to the wall thickness of 15 nm, without noticeable change in the length, SEM and TEM images of nanotube array being shown in Fig. 18. Annealed graphdiyne nanotube array shows high performance in field emission, as shown in Fig. 19 by comparing to nanotube before annealing and film¹⁰⁵. Loading of photocatalytic TiO_2 nanoparticles on graphdiyne nanosheet is shown to be effective to improve photoactivity, a little better than that on graphene^{113,114}. The cross-coupling reaction of hexaethynylbenzene was applied to synthesize nanowires of graphdiyne using ZnO nanorod arrays on a silicon substrate, the resultant nanowires had a conductivity of 1.9×10^3 S/m and a mobility of 7.1×10^2 cm^2/Vs at room temperature¹¹⁵. The polymer solar cell with the addition of 2.5 mass% graphdiyne exhibited an enhanced short circuit current to 2.4 mA/cm^2 and the highest power conversion efficiency of 3.52 %, which is 56 % higher than that of the cell without graphdiyne addition, probably due to high charge transport capability of graphdiyne and the formation of efficient percolation paths in the active layer¹¹⁶.

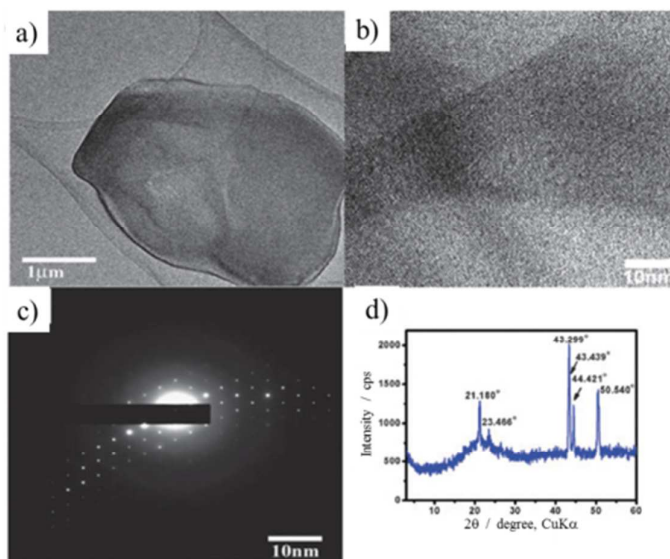


Fig. 17 TEM images (a and b), selected-area electron diffraction pattern (c) and XRD pattern (d) of graphdiyne film. Reproduced from ref. 111 with permission.

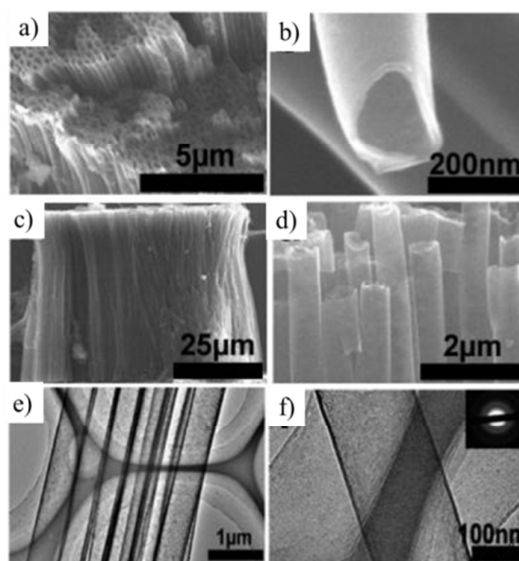


Fig. 18 Graphdiyne nanotube array after annealing: a) and b) top view, c) and d) side view by SEM, and e) and f) side view by TEM with inset of selected area electron diffraction pattern. Reproduced from ref. 112 with permission.

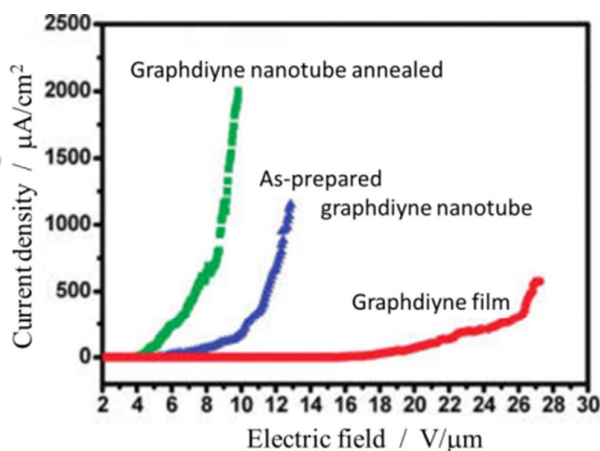


Fig. 19 Field emission performance of graphdiyne. Reproduced from ref. 112 with permission.

Theoretical consideration focusing on the properties related to the possible applications of graphyne and graphdiyne has been reported. In contrast to graphite where Li diffusion is confined in the interlayer space (in-plane diffusion), graphyne and graphdiyne can give a possibility for both in-plane and out-plane diffusion of Li ions, as illustrated on graphyne in Fig. 20, owing to the unique atomic arrangement and electronic structures¹¹⁷. Diffusion barriers calculated for two diffusion pathways are moderate, as 0.35-0.57 eV, and the maximum Li intercalation density can be LiC_4 in graphyne¹¹⁷, and LiC_3 in graphdiyne¹¹⁸, exceeding the limit of LiC_6 in graphite. Electronic properties of graphyne and graphdiyne nanoribbons with armchair and zigzag edges were discussed as a function of ribbon width^{119,120}. Band gap of these ribbons decreases with increasing ribbon width. Advantages of building p-n junctions based on graphyne were discussed¹²¹. The phonon thermal conductance of graphyne is much reduced, 46 % of graphene at room temperature, while it is larger than that of graphene at low temperatures because of the softer flexural

phonon modes in graphyne¹²². Due to the semiconductor property of graphyne, thermoelectric power was expected to be one magnitude larger than that of graphene. Thermal conductance showed a linear dependence on the width of armchair-edged graphyne nanoribbons, while step-like width dependence was displayed in the conductance of zigzag-edged nanoribbons¹²³.

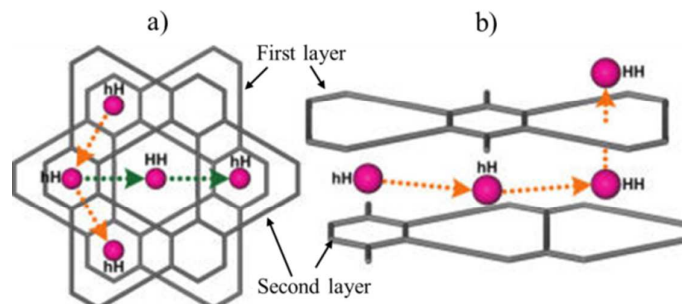


Fig. 20 In-plane diffusion pathway (a) and out-plane diffusion pathway (b) of Li in bulk graphyne. Reproduced from ref. 117 with permission.

The first-principles density functional calculations predicted that Ca-decorated graphyne can have high hydrogen-storage capacity as 6-8 mass% at 25 °C under 3 MPa¹²⁴⁻¹²⁶. Ca atoms are supposed to be highly dispersed on the surface of graphyne, although they tend to form clusters on the surface of graphene and fullerene. More hydrogen-storage capacity was predicted to Li-decorated graphyne, 9.26 mass% for single-side decorated and 15.15 mass% for both side decorated¹²⁷. Decoration effect of 3d transition metals (V, Cr, Mn, Fe, Co, and Ni) on electronic and magnetic properties of graphdiyne and graphyne was studied¹²⁸. Graphdiyne can serve as a separation membrane for H₂ purification from CH₄ and CO¹²⁹.

6. Concluding remarks

The present authors have proposed to classify the carbon materials on the basis of chemical bonds between carbon atoms, sp³, flat sp², curved sp² and sp¹ hybrid systems, and called diamond, graphite, fullerene and carbyne families, respectively^{130,131}. Graphite family involves a number of carbon materials, from classic carbons (represented by synthetic graphites, carbon blacks and activated carbons) and new carbons (represented by various carbon fibers, pyrolytic carbons, isotropic high-density graphites, etc.) to nanocarbons (represented by carbon nanotubes and graphenes). However, the development of graphyne and graphdiyne suggests us a new carbon family composed from two kinds of C-C bonds, sp² and sp¹. In addition, graphane, fluorographene and graphene oxide have to be included as new members of sp³ system. These carbon materials described in the present review can be derived whether by chemical reactions or theoretical considerations from graphene, as illustrated in Fig. 21. In the figure, fullerene and SWCNT, together with graphite and amorphous carbon, are included, because all of them can also be derived from graphene.

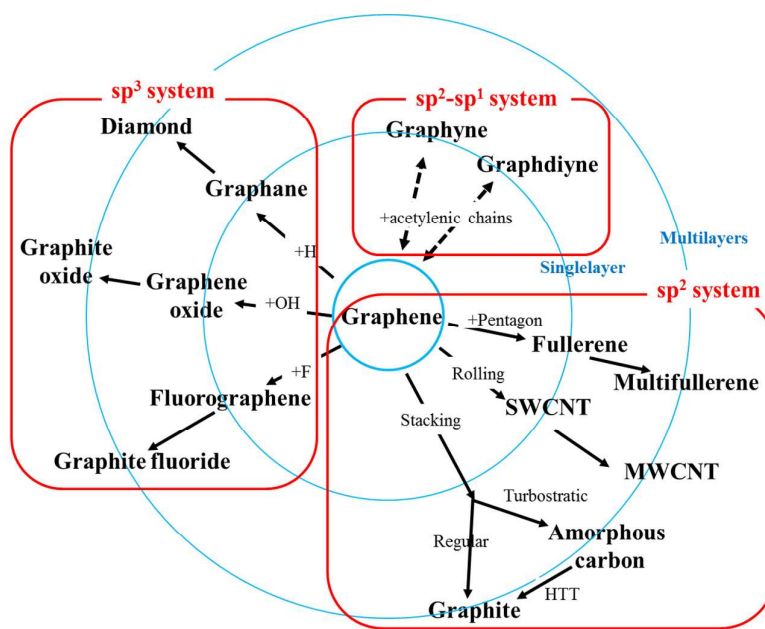


Fig. 21 Graphene derivatives

The chemical composition of graphane is CH , which may be considered as one of organic compounds with extremely large size, and may be giant hydrocarbon. Organic compounds, such as aromatic and aliphatic hydrocarbons including their mixtures as pitches, have been important precursors for all carbon materials. However, the development of graphene derivatives, as explained in the present review, graphene may be able to be an important starting material for giant organic compounds by introducing hydrogen as graphane and acetylenic linkages as graphyne and graphdiyne. The discovery of graphane and fluorographene may open the floodgates for new graphene-based nano-sized electronic elements, such as possible control in band-gap from zero-band-gap graphene to wide-band-gap graphane and fluorographene by partial hydrogenation and fluorination, nanoribbons with metallic graphene at one end and insulating graphene or fluorographene at the other end, graphane substituted foreign atoms, etc. Nanotubes of graphane and fluorographene are one-dimensional nanomaterials as predicted by theoretical consideration. The establishment in large-scale production processes for these materials in different morphologies, nanoflakes, nanoribbons and nanotubes is strongly demanded.

In addition to the derivatives reviewed here, porous graphene attracts attention because of its properties theoretically expected; extremely high selectivity on the order of 10^{23} for H_2/CH_4 on pore width of 0.25 nm^{132} , remarkably high selectivity for H_2/CO_2 , CO and CH_4 , and semiconductive behavior on postulated two-dimensional polyphenylene network¹³³, a large band gap of 3.2 eV , similar to photoactive TiO_2 and low energy for hydrogen adsorption after Li-decoration on two-dimensional polyphenylene network¹³⁴, and separating He from the other noble gases and alkanes present in natural gas¹³⁵. However, porous graphene, which was practically synthesized from hexaiodo-substituted macrocycle cyclohexa-*m*-phenylene by silver-promoted aryl-aryl coupling, contains various sizes of pores¹³⁶. Therefore, it is better to say heavily defective graphene, although it can be the first step for synthesis of porous graphene with controlled pores.

References

- 1 H. P. Boehm, R. Setton and E. Stumpp, *Carbon*, 1986, **24**, 241.
- 2 The 2010 Nobel Prize, http://nobelprize.org/nobel_prizes/physics/laureates/2010/press.html.

- 3 Editorial, *Carbon*, 2013, **65**, 1.
- 4 Q. Tang, Z. Zhou and Z. Chen, *Nanoscale*, 2013, **5**, 4541.
- 5 A. K. Geim and K. S. Novoselov, *Nat Mater*, 2007, **6**, 183; A. K. Geim, *Science*, 2009, **324**, 1530; C. Soldano, A. Mahmood and E. Dujardin, *Carbon*, 2010, **48**, 2127; M. J. Allen, V. C. Tung and R. B. Kaner, *Chem Rev*, 2010, **110**, 132; M. Terrones, A. R. Botello-Méndez, J. Campos-Delgado, F. López-Urías, Y. I. Vega-Cantú, F. J. Rodríguez-Macias, A. L. Elías, E. Muñoz-Sandoval, A. G. Cano-Márquez, J.-C. Charlier and H. Terrones, *Nano Today*, 2010, **5**, 351; M. Inagaki, Y. A. Kim and M. Endo, *J. Mater. Chem.*, 2011, **21**, 3280; X. Jia, J. Campos-Delgado, M. Terrones, V. Meunier and M. S. Dresselhaus, *Nanoscale*, 2011, **3**, 86; C. Zhang, W. Lv, X. Xie, D. Tang, C. Liu and Q.-H. Yang, *Carbon*, 2013, **62**, 11; C. Chung, Y.-K. Kim, D. Shin, S.-R. Ryoo, B.H. Hong and D.-H. Min, *Accounts Chem. Res.*, 2013, **46**, 2211.
- 6 M. H. F. Sluiter and Y. Kawazoe, *Phys. Rev. B*, 2003, **68**, 085410.
- 7 J. O. Sofó, A. S. Chaudhari, and G. D. Barber, *Phys. Rev. B*, 2007, **75**, 153401.
- 8 O. Leenaerts, H. Peelaers, A. D. Hernandez-Nieves, B. Partoens and F. M. Peeters, *Phys. Rev. B*, 2010, **82**, 195436.
- 9 M. Z. S. Flores, P. A. S. Autreto, S. B. Legoas and D. S. Galvao, *Nanotechnology*, 2009, **20**, 465704.
- 10 X. D. Wen, L. Hand, V. Labet, T. Yang, R. Hoffmann, N. W. Ashcroft, A. R. Oganov and A. O. Lyakhov, *Proc. Nat. Acad. Sci. USA*, 2011, **108**, 6833.
- 11 D. C. Elias, R. R. Nair, T. M. G. Mohiuddin, S. V. Morozov, P. Blake, M. P. Halsall, A. C. Ferrari, D. W. Boukhvalov, M. I. Katsnelson, A. K. Geim and K. S. Novoselov, *Science*, 2009, **323**, 610.
- 12 A. M. Ilyin, N. R. Guseinov, I. A. Tsyganov and R. R. Nemkaeva, *Physica E*, 2011, **43**, 1262.
- 13 M. Jaiswal, C. H. Y. X. Lim, Q. Bao, C. T. Toh, K. P. Loh and B. Ozyilmaz, *ACS Nano*, 2011, **5**, 888.
- 14 H. L. Poh, F. Z. Sanek, Z. Sofer and M. Pumera, *Nanoscale*, 2012, **4**, 7006.
- 15 H. L. Poh, Z. Sofer and M. Pumera, *Electrochem. Commun.*, 2012, **25**, 58.
- 16 J. Zhou, M. M. Wu, X. Zhou and Q. Sun, *Appl. Phys. Lett.*, 2009, **95**, 103108.
- 17 A. V. Talyzin, S. Luzan, I. V. Anoshkin, A. G. Nasibulin, H. Jiang, E. I. Kauppinen, V. M. Mikoushkin, V. V. Shnitov, D. E. Marchenko and D. Noréus, *ACS Nano*, 2011, **5**, 5132.
- 18 R. Balog, B. Jørgensen, L. Nilsson, M. Andersen, E. Rienks, M. Bianchi, M. Fanetti, E. Lægsgaard, A. Baraldi, S. Lizzit, Z. Slijivancanin, F. Besenbacher, B. Hammer, T.G. Pedersen, P. Hofmann, L. Hornekær, *Nat. Mater.*, 2010, **9**, 315.
- 19 S. Costamagna, M. Neek-Amal, J. H. Los and F. M. Peeters, *Phys. Rev. B*, 2012, **86**, 041408.
- 20 M. Neek-Amal and F. M. Peeters, *Phys. Rev. B*, 2011, **83**, 235437.
- 21 D. Vanzo, D. Bratko and A. Luzar, *J. Chem. Phys.*, 2012, **137**, 034707.
- 22 S. Lebègue, M. Klintonberg, O. Eriksson and M. I. Katsnelson, *Phys. Rev. B*, 2009, **79**, 245117.
- 23 H. Sahin, C. Ataca and S. Ciraci, *Phys. Rev. B*, 2010, **81**, 205417.
- 24 J. Zhou, Q. Wang, Q. Sun, X. S. Chen, Y. Kawazoe and P. Jena, *Nano Lett.* 2009, **9**, 3867.
- 25 J. Berashevich and T. Chakraborty, *Nanotechnol*, 2010, **21**, 355201.
- 26 A. D. Hernandez-Nieves, B. Partoens and F. M. Peeters, *Phys. Rev. B*, 2010, **82**, 165412.
- 27 T. Hussain, B. Pathak, T. A. Maark, M. Ramzan and R. Ahuja, *EPL*, 2012, **99**, 47004.
- 28 P. Cudazzo, C. Attaccalite, I. V. Tokatly and A. Rubio, *Phys. Rev. Lett.*, 2010, **104**, 226804.
- 29 Y. Wang, Y. Ding, S. Shi and W. Tang, *Appl. Phys. Lett.*, 2011, **98**, 163104.
- 30 T. Hussain, B. Pathak, T. A. Maark, C. M. Araujo, R. H. Scheicher and R. Ahuja, *EPL*, 2011, **96**, 27013.
- 31 M. Khazaei, M. S. Bahramy, N. S. Venkataramanan, H. Mizuseki and Y. Kawazoe, *J. Appl. Phys.*, 2009, **106**, 094303.
- 32 X. D. Wen, T. Yang, R. Hoffmann, N. W. Ashcroft, R. L. Martin, S. P. Rudin and J. X. Zhu, *ACS Nano*, 2012, **6**, 7142.
- 33 Y. Li, Z. Zhou, P. Shen and Z. Chen, *J. Phys. Chem. C*, 2009, **113**, 15043.
- 34 O. Ruff and O. Bretschneider, *Z. Anorg. Allg. Chem.*, 1934, **217**, 1.
- 35 W. Rüdorff and G. Rüdorff, *Chem. Ber.*, 1947, **80**, 413.
- 36 H. Touhara, K. Kakuno and N. Watanabe, *TANSO*, 1984, **No. 117**, 98 [in Japanese]; N. Watanabe, T. Nakajima and H. Touhara, *Graphite Fluorides*. Elsevier, Amsterdam, 1988; T. Nakajima and N. Watanabe, *Graphite Fluorides and Carbon-Fluorine Compounds*. CRC, Boca Raton, FL, 1991.
- 37 R. R. Nair, W. Ren, R. Jalil, I. Riaz, V. G. Kravets, L. Britnell, P. Blake, F. Schedin, A. S. Mayorov, S. Yuan, M. I. Katsnelson, H. M. Cheng, W. Strupinski, L. G. Bulusheva, A. V. Okotrub, I. V. Grigorieva, A. N. Grigorenko, K. S. Novoselov and A. K. Geim, *Small*, 2010, **6**, 2877.
- 38 J. T. Robinson, J. S. Burgess, C. E. Junkermeier, S. C. Badescu, T. L. Reinecke, F. K. Perkins, M. K.

- Zalautdniov, J. W. Baldwin, J. C. Culbertson, P. E. Sheehan and E. S. Snow, *Nano Lett.*, 2010, **10**, 3001.
- 39 K. J. Jeon, Z. Lee, E. Pollak, L. Moreschini, A. Bostwick, C-M. Park, R. Mendelsberg, V. Radmilovic, R. Kostecki, T. J. Richardson and E. Rotenberg, *ACS Nano*, 2011, **5**, 1042.
- 40 X. Hong, S. H. Cheng, C. Herding and J. Zhu, *Phys. Rev. B*, 2011, **83**, 085410.
- 41 R. Zbořil, F. Karlický, A. B. Bourlinos, T. A. Steriotis, A. K. Stubos, V. Georgakilas, K. Šafařová, D. Jančík, C. Trapalis and M. Otyepka, *Small*, 2010, **6**, 2885.
- 42 H. Chang, J. Cheng, X. Liu, J. Gao, M. Li, J. Li, X. Tao, F. Ding and Z. Zheng, *Chem. Eur. J.*, 2011, **17**, 8896.
- 43 P. Gong, Z. Wang, J. Wang, H. Wang, Z. Li, Z. Fan, Y. Xu, X. Han and S. Yang, *J. Mater. Chem.*, 2012, **22**, 16950.
- 44 Z. Wang, J. Wang, Z. Li, P. Gong, X. Liu, L. Zhang, J. Ren, H. Wang and S. Yang, *Carbon*, 2012, **50**, 5403.
- 45 O. Leenaerts, H. Peelaers, A. D. Hernandez-Nieves, B. Partoens and F. M. Peeters, *Phys. Rev. B*, 2010, **82**, 195436.
- 46 A. Markevich, R. Jones and P. R. Briddon, *Phys. Rev. B*, 2011, **84**, 115439.
- 47 S. Tang and S. Zhang, *J. Phys. Chem. C*, 2011, **115**, 16644.
- 48 D. K. Samarakoon, Z. Chen, C. Nicolas and X. Q. Wang, *Small*, 2011, **7**, 965.
- 49 O. Leenaerts, H. Sahin, B. Partons and F. M. Peeters, *Phys. Rev. B*, 2013, **88**, 035434.
- 50 L. F. Wang, T. B. Ma, Y. Z. Hu, H. Wang and T. M. Shao, *J. Phys. Chem. C*, 2013, **117**, 12520.
- 51 R. Pauptiz, P. A. S. Autreto, S. B. Legoas, S. G. Srinivasan, T. van Duin and D. S. Galvao, *Nanotechnol.*, 2013, **24**, 035706.
- 52 E. T. Mickelson, C. B. Huffman, A. G. Rinzler, R. E. Smalley, R. H. Hauge and J. L. Margrave, *Chem. Phys. Lett.*, 1998, **296**, 188.
- 53 R. L. Vander Wal, K. Miyoshi, K. W. Street, A. J. Tomasek, H. Peng, Y. Liu, J. L. Margrave and V. N. Khabashesku, *Wear* 2005, **259**, 738.
- 54 W. S. Hummers and R. E. Offeman, *J. Am. Chem. Soc.*, 1958, **80**, 1339.
- 55 L. Staudenmaier, *Ber. Dtsch. Chem. Ges.*, 1898, **31**, 1481.
- 56 B. C. Brodie, *Ann. Chim. Phys.*, 1860, **59**, 466.
- 57 F. Kang, Y. Leng and T-Y. Zhang, *Carbon*, 1997, **35**, 1089-96.
- 58 M. Toyoda, A. Shimizu, H. Iwata and M. Inagaki, *Carbon*, 2001, **39**, 1697.
- 59 W-G. Weng, G-H. Chen, D-J. Wu, Z-Y. Lin and W-L. Yan, *Synth. Met.* 2003, **139**, 221.
- 60 D. C. Marcano, D. V. Kosynkin, J. M. Berlin, A. Sinitskii, Z. Sun, A. Slesarev, L. B. Alemany, W. Lu and J. M. Tour, *ACS Nano*, 2010, **4**, 4806.
- 61 A. M. Dimiev and J. M. Tour, *ACS Nano*, 2014, **8**, 3060.
- 62 W. Schloz and H. P. Boehm, *Z. Anorg. Allg. Chem.*, 1969, **369**, 327.
- 63 R. Yazami, Ph. Touzain, Y. Chabre, D. Berger and M. Coulon, *Rev. Chim. Minerale*. 1985, **22**, 398.
- 64 T. Nakajima and Y. Matsuo, *Carbon*, 1994, **32**, 469.
- 65 T. Szabó, O. Berkesi, P. Eorgó, K. Josepovits, Y. Sanakis, D. Petridis and I. Dékány, *Chem. Mater.*, 2006, **18**, 2740.
- 66 I. Dékány, R. Küger-Grasser and A. Weiss, *Colloid. Polym. Sci.*, 1998, **276**, 570.
- 67 Y. Matsuo, T. Niwa and Y. Sugie, *Carbon*, 1999, **37**, 897.
- 68 Y. Matsuo, K. Hatase and Y. Sugie, *Chem. Lett.*, 1999, 1109.
- 69 Z. Liu, Z. Wang, X. Yang and K. Ooi, *Langmuir*, 2002, **18**, 4926.
- 70 J. W. Burrell, S. Gadipelli, J. Ford, J. M. Simmons, W. Zhou and T. Yildirim, *Angew. Chem. Int. Ed.*, 2010, **49**, 8902.
- 71 D. R. Dreyer, S. Park, C. W. Bielawski and R. S. Ruoff, *Chem. Soc. Rev.*, 2010, **39**, 228.
- 72 S. Kim, S. Zhou, Y. Hu, M. Acik, Y. J. Chabal, C. Berger, W. de Heer, A. Bongiorno and E. Riedo, *Nat. Mater.*, 2012, **11**, 544.
- 73 K. A. Mkhoyan, A. W. Contryman, J. Silcox, D. A. Stewart, G. Eda, C. Mattevi, S. Miller and M. Chhowalla, *Nano Lett.*, 2009, **9**, 1058.
- 74 D. Dikin, S. Stankovich, E. J. Zimney, R. D. Piner, G. H. B. Dommett, G. Evmenenko, S. T. Nguyen and R. S. Ruoff, *Nature* 2007, **448**, 457.
- 75 C. Gomez-Navarro, R. T. Weitz, A. M. Bittner, M. Scolari, A. Mews, M. Burghard and K. Kern, *Nano Lett.*, 2007, **7**, 3499.
- 76 X. Li, G. Zhang, X. Bai, X. Sun, X. Wang, E. Wang and H. Dai, *Nat. Nanotechnol.*, 2008, **3**, 538.
- 77 Y. Zhu, S. Murali, W. Cai, X. Li, J. W. Suk, J. R. Potts and R. S. Ruoff, *Adv. Mater.*, 2010, **22**, 3906.

- 78 I. K. Moon, J. Lee, R. S. Ruoff and H. Lee, *Nat. Commun.*, 2010, **1**, 73
- 79 Z. Wei, D. Wang, S. Kim, S. Y. Kim, Y. Hu, M. K. Yakes, A. R. Laracuenta, Z. Dai, S. R. Marder, C. Berger, W. P. King, W. A. de Heer, P. E. Sheehan and E. Riedo, *Science*, 2010, **328**, 1373
- 80 J. Zhao, S. Pei, W. Ren, L. Gao, and H. M. Cheng, *ACS Nano*, 2010, **4**, 5245.
- 81 S. Pei and H. M. Cheng, *Carbon*, 2012, **50**, 3210.
- 82 S. Stankovich, R. D. Piner, X. Chen, N. Wu, S. B. T. Nguyen and R. S. Ruoff, *J. Mater. Chem.*, 2006, **16**, 155.
- 83 I. Jung, D. A. Dikin, R. D. Piner and R. S. Ruoff, *Nano Lett.*, 2008, **8**, 4283.
- 84 P. Johari and V. B. Shenoy, *ACS Nano*, 2011, **5**, 7640.
- 85 Y. Cao, Y. Chong, H. Shen, M. Zhang, J. Huang, Y. Zhu and Z. Zhang, *J. Mater. Chem. B*, 2013, **1**, 5602.
- 86 L. Feng, X. Yang, X. Shi, X. Tan, R. Peng, J. Wang and Z. Liu, *Small*, 2013, **9**, 1989.
- 87 X. Shi, H. Gong, Y. Li, C. Wang, L. Cheng and Z. Liu, *Biomater.*, 2013, **34**, 4786.
- 88 K. Yang, L. Z. Feng, X. Z. Shi and Z. Liu, *Chem. Soc. Rev.*, 2013, **42**, 530.
- 89 E. Morales-Narváez and A. Merkoci, *Adv. Mater.*, 2012, **24**, 3298.
- 90 R. H. Baughman, H. Eckhardt and M. J. Kertesz, *J. Chem. Phys.*, 1987, **87**, 6687.
- 91 M. M. Haley, S. C. Brand and J. J. Pak, *Angew. Chem. Int. Ed.*, 1997, **36**, 836.
- 92 N. Narita, S. Nagagi, S. Suzuki and K. Nakao, *Phys. Rev. B*, 1998, **58**, 11009.
- 93 M. M. Haley, *Pure Appl. Chem.*, 2008, **80**, 519.
- 94 A. L. Ivanovskii, *Prog. Solid State Chem.*, 2013, **41**, 1.
- 95 M. Long, L. Tang, D. Wang, Y. Li and Z. Shuai, *ACS Nano*, 2011, **5**, 2593.
- 96 J. Kang, J. Li, F. Wu, S. S. Li and J. B. Xia, *J. Phys. Chem. C*, 2011, **115**, 20466.
- 97 Q. Peng, W. Ji and S. De, *Phys. Chem. Phys.*, 2012, **14**, 13385.
- 98 G. Luo, Q. Zheng, W. N. Mei, J. Lu and S. Nagase, *J. Phys. Chem. C*, 2013, **117**, 13072.
- 99 Y. Y. Zhang, Q. X. Pei and C. M. Wang, *Comp. Mater. Sci.*, 2012, **65**, 406.
- 100 S. W. Cranford and M. J. Buehler, *Carbon*, 2011, **49**, 4111.
- 101 S. W. Cranford, D. B. Brommer and M. J. Buehler, *Nanoscale*, 2012, **4**, 7797.
- 102 Y. Y. Zhang, Q. X. Pei and C. M. Wang, *Appl. Phys. Lett.*, 2012, **101**, 081909
- 103 W. B. Wan, S. C. Brand, J. J. Pak and M. M. Haley, *Chem. Eur. J.*, 2000, **6**, 2044.
- 104 J. M. Kehoe, J. H. Kiley, J. J. English, C. A. Johnson, R. C. Petersen and M. M. Haley, *Org. Lett.*, 2000, **2**, 969.
- 105 W. B. Wan and M. M. Haley, *J. Org. Chem.*, 2001, **66**, 3893.
- 106 J. A. Marsden, G. J. Palmer and M. M. Haley, *Eur. J. Org. Chem.*, 2003, **23**, 2355.
- 107 J. A. Marsden and M. M. Haley, *J. Org. Chem.*, 2005, **70**, 10213.
- 108 K. Tahara, T. Yoshimura, M. Sonoda, Y. Tobe and R. V. Williams, *J. Org. Chem.*, 2007, **72**, 1437.
- 109 M. M. Haley, *Pure Appl. Chem.*, 2008, **80**, 519.
- 110 E. L. Spitler, J. M. Monson and M. M. Haley, *J. Org. Chem.*, 2008, **73**, 2211.
- 111 G. Li, Y. Li, H. Liu, Y. Guo, Y. Li and D. Zhu, *Chem. Commun.*, 2010, **46**, 3256.
- 112 G. Li, Y. Li, X. Qian, H. Liu, H. Lin, N. Chen and Y. Li, *J. Phys. Chem. C*, 2011, **115**, 2611.
- 113 S. Wang, L. Yi, J. E. Halpert, X. Lai, Y. Liu, H. Cao, R. Yu, D. Wang and Y. Li, *Small*, 2012, **8**, 265.
- 114 N. Yang, Y. Liu, H. Wen, Z. Tang, H. Zhao, Y. Li and D. *ACS Nano*, 2013, **7**, 1504.
- 115 X. Qian, Z. Ning, Y. Li, H. Liu, C. Ouyang, Q. Chen and Y. Li, *Dalton Trans.*, 2012, **41**, 730.
- 116 H. Du, Z. Deng, Z. Lv, Y. Yin, L. Yu, H. Wu, Z. Chen, Y. Zou, Y. Wang, H. Liu and Y. Li, *Synth. Met.*, 2011, **161**, 2055.
- 117 H. Zhang, M. Zhao, X. He, Z. Wang, X. Zhang and X. Liu, *J. Phys. Chem. C*, 2011, **115**, 8845.
- 118 H. Zhang, Y. Xia, H. Bu, X. Wang, M. Zhang, Y. Luo and M. Zhao, *J. Appl. Phys.*, 2013, **113**, 044309.
- 119 L. D. Pan, L. Z. Zhang, B. Q. Song, S. X. Du and H. J. Gao, *Appl. Phys. Lett.*, 2011, **98**, 173102.
- 120 H. Bai, Y. Zhu, W. Qiao and Y. Huang, *RSC Adv.*, 2011, **1**, 768.
- 121 T. Ouyang, H. Xiao, Y. Xie, X. Wei, Y. Chen and J. Zhong, *J. Appl. Phys.*, 2013, **114**, 073710.
- 122 X. M. Wang, D. C. Mo and S. S. Lu, *J. Chem. Phys.*, 2013, **138**, 204704.
- 123 T. Ouyang, Y. Chen, L-M. Liu, Y. Xie, X. Wei and J. Zhong, *Phys. Rev. B*, 2012, **85**, 235436.
- 124 C. Li, J. Li, F. Wu, S. S. Li, J. B. Xia, and L. W. Wang, *J. Phys. Chem. C*, 2011, **115**, 23221.
- 125 H. J. Hwang, Y. Kwon and H. Lee, *J. Phys. Chem. C*, 2012, **116**, 20220.
- 126 Y. S. Wang, P. F. Yuan, M. Li, W. F. Jiang, Q. Sun and Y. Jia, *J. Solid State Chem.*, 2013, **197**, 323.
- 127 H. Zhang, M. Zhao, H. Bu, X. He, M. Zhang, L. Zhao and Y. Luo, *J. Appl. Phys.*, 2012, **112**, 084305.
- 128 J. He, S. Y. Ma, P. Zhou, C. X. Zhang, C. He and L. Z. Sun, *J. Phys. Chem. C*, 2012, **116**, 26313.
- 129 Y. Jiao, A. Du, M. Hankel, Z. Zhu, V. Rudolph and S. C. Smith, *Chem. Commun.*, 2011, **47**, 11843.

- 130 M. Inagaki, *New Carbons - Control of Structure and Functions*. Elsevier, 2000.
- 131 M. Inagaki and F. Kang, *Carbon Materials Science and Engineering - From fundamentals to Applications*. Tsinghua University Press, 2006.
- 132 D. Jiang, V. R. Cooper and S. Dai, *Nano Lett.*, 2009, **9**, 4019.
- 133 Y. Li, Z. Zhou, P. Shen and Z. Chen, *Chem. Commun.*, 2010, 3672.
- 134 A. Du, Z. Zhu and S. C. Smith, *J. Am. Chem. Soc.*, 2010, **132**, 2876.
- 135 J. Schrier, *J. Phys. Chem. Lett.*, 2010, **1**, 2284.
- 136 M. Bieri, M. Treier, J. Cai, K. Ait-Mansour, P. Ruffieux, O. Groning, P. Groning, M. Kastler, R. Rieger, X. Feng, K. Mullen and R. Fasel, *Chem. Commun.* 2009, 6919.